

CHAPTER V - SECONDARY BEAM LINES

1. INTRODUCTION

The task of the Secondary Beam Lines Section is to define a system that selects and transports a radioactive species extracted from the ion source to the experimental areas. These areas are:

- (a) the existing GANIL areas reached after charge-breeding via post-acceleration in the CIME cyclotron, and
- (b) a new low-energy physics area (Figure 1). These two lines should be fed simultaneously (with separated ion species).

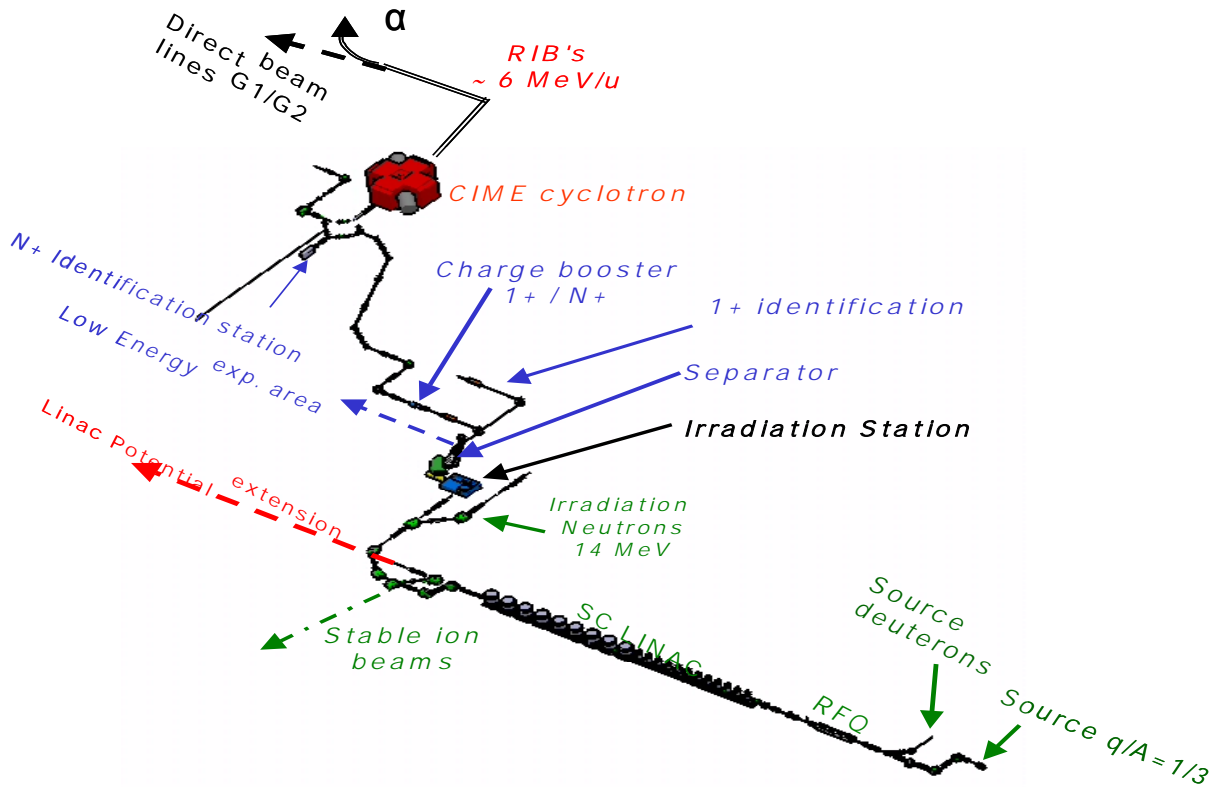


Figure 1: Schematic layout of SPIRAL 2

The following requirements and constraints have to be taken into account:

- Singly-charged beams from an ECR source with high output current and large emittance
- Selective ion sources with low-emittance, low-current beams: typical beams produced by various different ions sources are listed below:

Source of 1+ ions	Beam quality	Typical beams produced
Surface ionisation	$<10\pi$ mm.mrad, 100 μ A	^8Li , K, Na; $^{92,96}\text{Rb}$, $^{142,148}\text{Cs}$
ECR	$40-80\pi$ mm.mrad, 2-5 mA	$^{8,6}\text{He}$, $^{24,26}\text{Ne}$, $^{46\dots}\text{Ar}$; $^{92,96}\text{Kr}$; $^{142,148}\text{Xe}$
Laser	$<10\pi$ mm.mrad, 100 μ A	Surface ionisation beam: +1 element laser-ionised
Hot plasma	$40-80\pi$ mm.mrad, 2 mA	Not selective

- Large mass acceptance bi-directional separator
- Charge breeder required by the acceleration in the CIME cyclotron
- Extremely high radiation environment (see Chapter IX on Safety, and Table 1 below)
- Personal safety to be ensured and spreading of radioactive material to be made impossible.

Table 1 gives an estimate of the radioactivity produced at different locations in the secondary beam lines.

Table 1: Radioactivity estimates for a 3-month irradiation of 5 kg of ^{238}U by 5 mA of 40-MeV deuterons

	Bq	Ci	Sv/h @ 1 m	Remarks
Target	$5.6 \cdot 10^{14}$	15 000	61	
TIS exit	$3.0 \cdot 10^{14}$	8 000	30	\approx losses inside separator
Separator exit	$1.0 \cdot 10^{13}$	300	2.6	\approx losses inside breeder
Breeder exit	$5.0 \cdot 10^{11}$	15	0.1	$\frac{1}{2} \approx$ losses inside CIME
CIME exit	$2.0 \cdot 10^{11}$	5	0.1	\approx losses on target inside GANIL

2. THE SEPARATOR

The device must separate fission products extending roughly from mass 70 to 160. The full current intensity to be taken into account at the exit of the source and entering into the separator can be as high as 5 mA and its emittance as large as 80π mm.mrad (see chapter IV). The mass resolution to be reached has been fixed at $R=250$ and the mass difference between the two channels, i.e. to CIME cyclotron and low energy beam line respectively, at less than or equal to 15 mass units.

To fulfil the requirements of simultaneous beams, two devices have been investigated, one in the earlier part of the APD study, called BRAMA, and a second, in the latter half of the study, based on a Wien filter.

(a) The BRAMA type solution [1] (Figure 2) is based on an Elbek magnet [2] and sliding electrostatic deflectors, which can deliver any mass to any channel. It is compact but complex. As will be described, one of the major drawback of the Elbek-based solution is the low transmission for high beam current, due to space charge forces: thus the well-defined object point – which is needed to ensure the BRAMA optical properties – cannot be maintained in this case. The proposed solution to this problem is to include a section equipped with dipole magnets prior to the Elbek spectrometer that will bend the high-current, low-mass beams from the ECR away from the object point, at the expense of added length and complexity.

As part of this study, a completely static magnetic solution, called Bi-Selective, of equivalent size than the Brama separator was also considered [3]. This solution favours the heaviest masses to one beam line and the lowest one to the other. To invert this, a simple switching matrix is required inside downstream beam lines. The detailed study of this solution is however not yet finalized.

(b) The Wien filter solution: a preliminary study had shown that it was very attractive, mainly because of the suppression of the space charge problem, insofar as the optics of such a device does not require a focused object point. We therefore decided to study it in more detail.

Two main options are thus presented below: the BRAMA and the Wien filter options. As mentioned earlier, safety considerations are of paramount importance: the nuclear engineering company which has been contracted will study the maintenance implications for both solutions. The final choice of the separator will be made after their conclusions are available.

The layouts presented below should not be viewed as final, as inputs from the nuclear engineering company are essential and will most probably need the beam lines to be rearranged in order to take the safety requirements into account. These layouts include almost all the elements that these beam lines should contain, with the exception of all the safety, access and ancillary requirements, but they do fulfil the optical specifications and represent a good starting point. In parallel, a risk analysis has been performed on all subsystems in preparation for discussions with the nuclear engineering company.

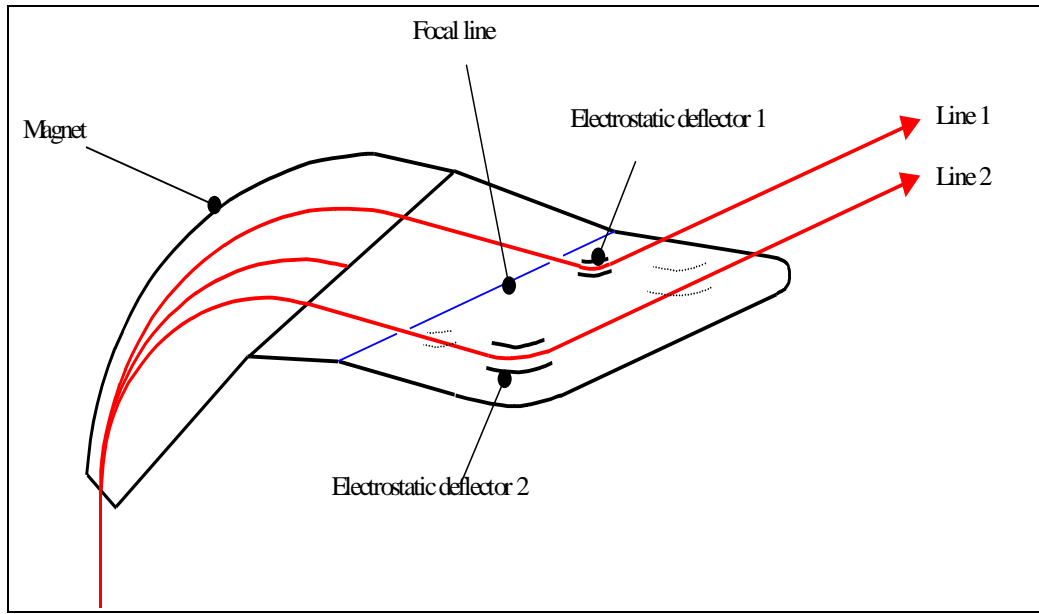


Figure 2: The BRAMA option.

2.1. BRAMA OPTION

2.1.1. Source-separator beam section (LSS beam line)

The source-separator beam line has to transport simultaneously all single-charge species extracted from the source and to realize beam optical parameters at the object focal point of the separator for the selected masses. We propose to build it into a number of ‘plug’ structures, similar to that of the target/ion-source system, in order to make maintenance easier (as in the TRIUMF/ISAC facility). This line must be as short as possible to reduce localized beam-loss areas and hence is composed of electrostatic elements only. For the design of this line, the conditions corresponding to the ECR source have been taken into account, as they correspond to the highest beam emittance and, at the same time, the highest beam intensity expected (up to 5 mA total intensity, due essentially to the presence of light ions from the support gas of the ECR source and from the out-gassing of the target).

A preliminary, very compact design was first developed to evaluate its transmission limits with regard to space charge effects. Finally, a second, improved design, including a pre-analyser structure, has been made to respect the contractual specifications of the system. The two next subsections summarize our studies.

2.1.1.a. Basic version of LSS beam line

To perform correctly, the BRAMA separator must receive a perfectly matched beam at its object focal point. Space charge effects at its entrance cause deterioration of this focusing, and therefore to obtain a good image point requires good mass-selection of desired ion species only.

The main concept of this basic version is a short beam line able to be placed into a low-energy plug (or plugs) and to perform the betatron matching needed by the BRAMA separator, as well as beam emittance matching to the acceptance of downstream lines (fixed at 80π mm.mrad).

From the optical point of view, the four betatron functions to be fulfilled at the object point of the separator are realized by using one einzel lens, located just after the source, and a set of three electrostatic quadrupoles located just at the beginning of the low-energy plug. A second plug is occupied by a collimator that provides the optimal definition of optical conditions. This collimator is a block of carbon in which the optimum profile of the beam is machined. It is movable vertically so that, at its withdrawn position, it forms a beam stop. Figure 3 shows this double plug system.

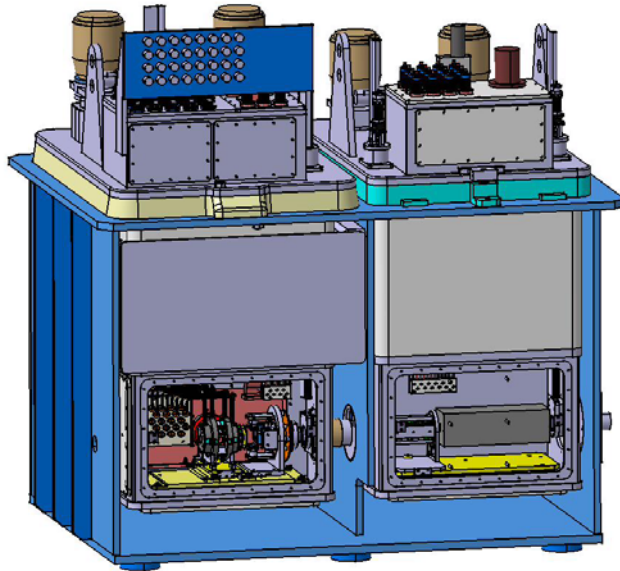


Figure 3: Mechanical view of the two plugs.

However, the use of an ECR source to produce singly-charged ions beam for SPIRAL 2 presents a major drawback for this type of structure. In addition to the required ion species produced in the target (i.e. between masses 70 and 160), a high intensity of light ions – essentially from the support gas of the source – is also extracted. In normal operation, we estimate that this type of source is able to provide a few milliamps of singly-charged ions. Working at low voltage (10 to 60 kV), space charge effects predominate for obtaining desired optical conditions at the object point. Figure 4 shows the first-order optics we obtain with this structure with characteristic intensities.

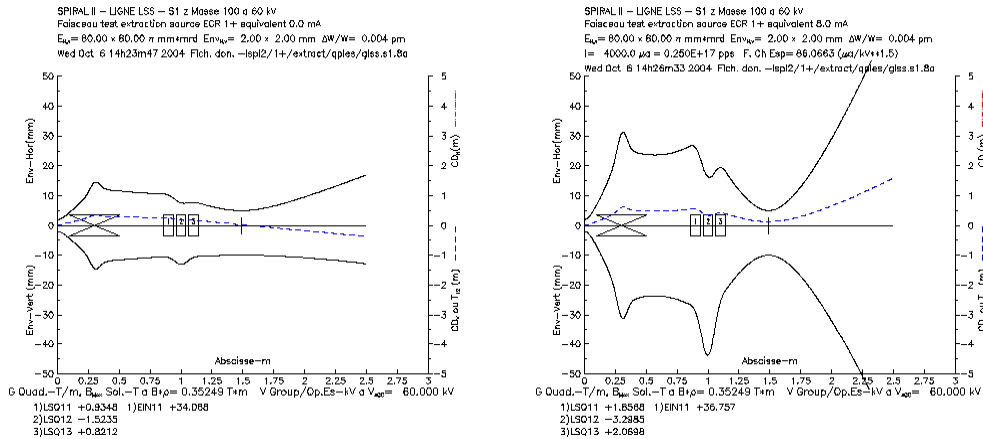


Figure 4: LSS line optics for 0 mA and 8 mA at 60 kV

Multi-particle calculations show that taking into account intensity and space charge effects lead to unacceptable aberrations and to a drastic limitation of the line transmission. Figure 5 presents beam envelopes and transverse phase projections obtained at the object point before emittance cutting and at the entrance of the separator after emittance cutting.

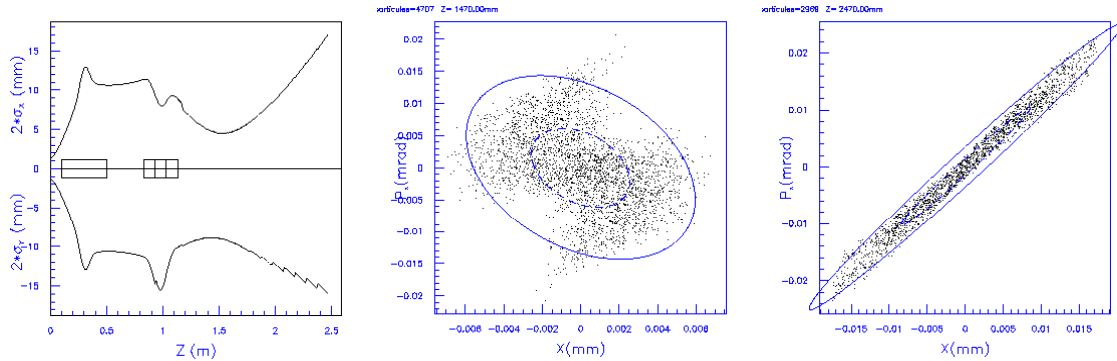


Figure 5: Multi-particle calculation results for 1 mA at 60 kV.

Beam transmissions through the structure as function of total intensity extracted from the ECR source are summarized in Table 2.

Table 2: Transmissions of LSS initial structure in function of intensity (equivalent space charge effects)

Beam intensity at 60 kV	Beam intensity at 30 kV	Beam intensity at 15 kV	Transmission to object point	Emittance growth	Transmission after emittance cutting
0 mA	0 mA	0 mA	100%	0%	100%
1 mA	0.354 mA	0.125 mA	94%	+ 50%	52%
2 mA	0.706 mA	0.250 mA	84%	+ 100%	16%
4 mA	1.412 mA	0.500 mA	63%	+ 220%	5%
6 mA	2.120 mA	0.750 mA	52%	+ 330%	-
8 mA	2.824 mA	1 mA	40%	+ 450%	-

It appears unrealistic to use this type of structure to transport and match the low-energy beam from an ECR source in condition of high intensity. Nevertheless, its compactness is very interesting from a safety viewpoint.

2.1.1.b. LSS beam line including pre-analyser

To overcome the space charge problem for injecting all radioactive species of interest for SPIRAL 2 beams correctly, a pre-analyser system has been implemented upstream of the BRAMA separator. It is composed of an achromatic double bend, designed to suppress light ions and recombine all mass-70 to mass-160 species into a unique beam before the object point of the separator. In this way, betatron matching from this focal point can be performed in the absence of space charge.

Implementation of all this new structure is now being studied to evaluate its suitability for insertion in a plug structure. Figure 6 shows the status of art of this development.

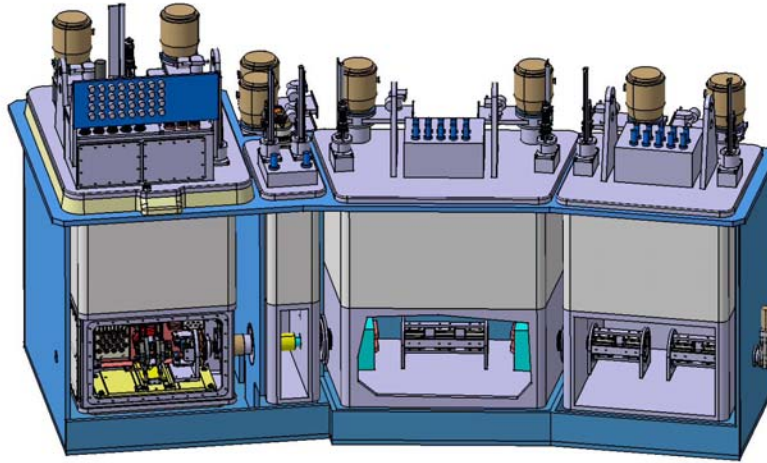


Figure 6: LSS line, new low-energy plug structure.

This LSS line is optically divided in three parts. Two einzel lenses constitute the first one. The first lens directly controls the beam extracted from the source and the second achieves the beam matching for the achromatic double bend. In this way, the source beam characteristics are relatively well dissociated from those of the double bend. The second section is the achromatic double bend itself. It is composed of two small magnetic dipoles located symmetrically on either side of three electrostatic quadrupoles. The third section, using four electrostatic quadrupoles, performs the betatron matching to the beam conditions required by the separator at its object point. Figure 7 shows the first-order optics obtained with two characteristic intensities.

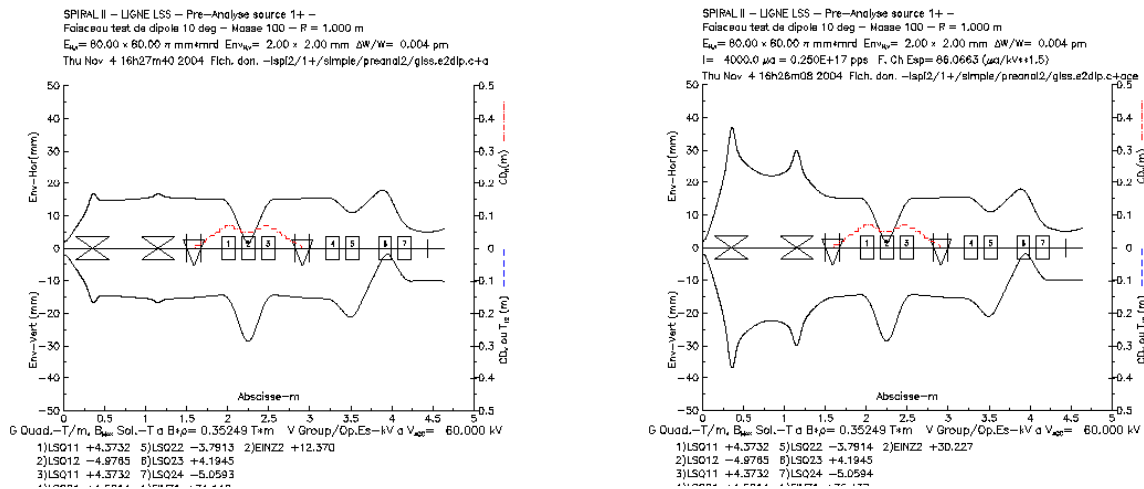


Figure 7: LSS line optics for 0 mA and 8 mA at 60 kV.

These calculations assume a linear decrease of space charge forces during the passage through the first magnetic dipole. In this double-bend system, particles with the masses of interest are separated and then re-unified. Figure 8 and Figure 9 show the XY projection in the middle and at the end of its for masses 70, 100 and 160 when dipoles are set for mass 100.

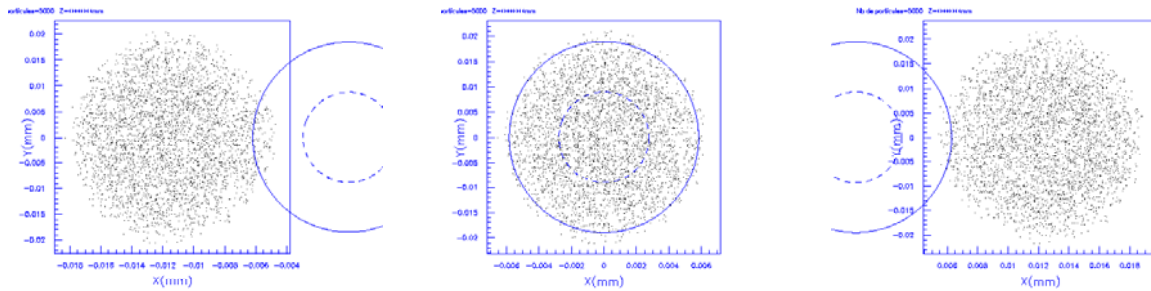


Figure 8: XY-plane in the middle of the double bend for masses 70, 100 and 160

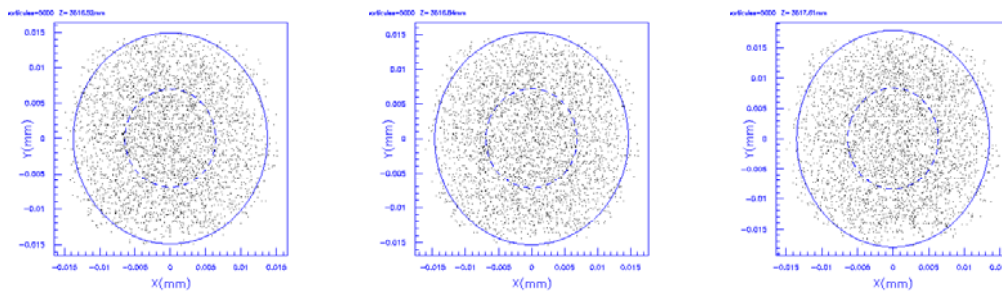


Figure 9: XY-plane at the end of the double bend for masses 70, 100 and 160

2.1.2. BRAMA Spectrometer

2.1.2.a. Updated mechanical design

A preliminary design of the BRAMA separator was made in November 2003. The main advantages of the solution were the complete stopping of unwanted beams in the focal plane, and the use of “off the shelf” mechanical components. However, the system had several known drawbacks, such as the use of four independent motors to drive the slits and deflectors separately, adding to the complexity of the system and also the difficulty of extracting the system from the chambers.

Several factors led to major changes in the design. One of the most important modifications came from the need to be able to service the equipment inside the chambers in case of failure. As the high level of contaminants inside the chambers precludes opening them to the ambient, all the components inside the chambers have been gathered onto a single platform that can be extracted as a unit from the separator. This operation is made possible thanks to a mobile airlock chamber that will be connected to a face of the deflector chamber. Two large valves, placed on each chamber, will allow the transfer of the platform to the inside of the mobile chamber without any spread of contaminants into the separator room. The faulty equipment would then be transferred to a hot cell for possible repair.

The basic principals of this solution are shown in the Figure 10.

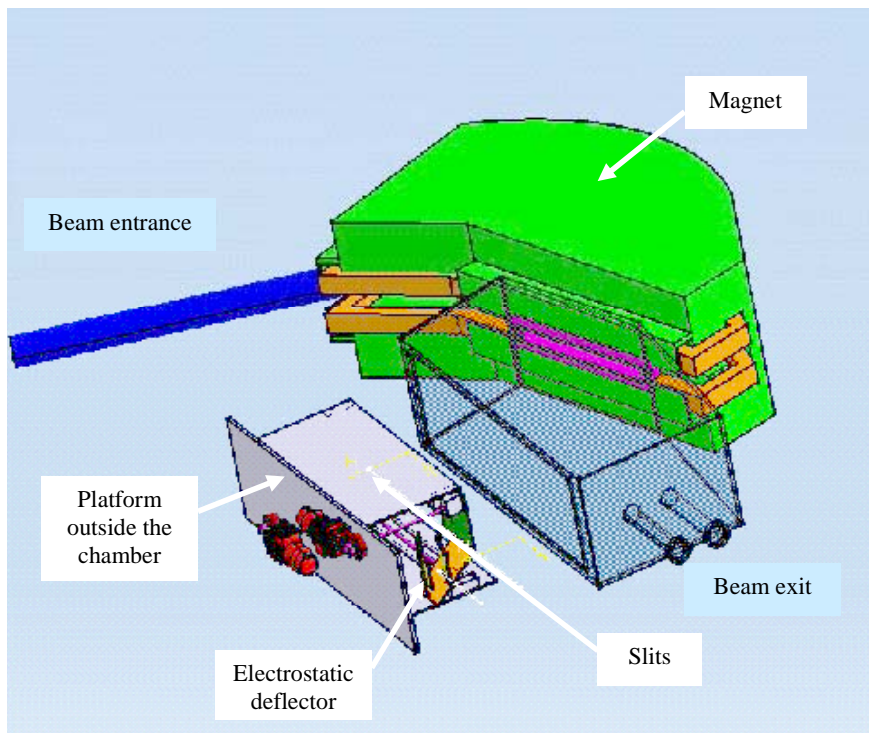


Figure 10: Updated mechanical setup of the BRAMA separator.

The new configuration shows a higher level of reliability and servicing, while maintaining its properties, delivering two simultaneous beams in a mass range from 70 to 160, the minimum range between selected species being 15 mass units, due to the physical size of the slit/deflector assembly. Slits and deflectors are interdependent, which allows the use of two motors instead of four as in the previous setup. Also, the space around the exit pipes has been freed from the mechanical rods formerly needed to drive motions inside the chambers. Slit heating due to beam spot impact has been evaluated in order to define the thermal stresses applied to connected components and it has been found that no cooling is needed.

The main disadvantages are a significant increase in the deflector chamber width, and the use of additional components inside the chambers. Indeed the first solution made use of long rods to translate either the deflectors or the slits along the focal line. In this design, two 90° angle-gearboxes, each connected to a worm screw, are placed inside the deflector chamber to drive the motions of the two carts holding the slits and the deflectors. Though it is not yet clear how long this system can work without any servicing, good results have been reported from analogous separators which exist as the GPS at ISOLDE [4,5,6], but some periodical maintenance might be needed in normal use. The frequency of such maintenance should remain low owing to the low level of the mechanical constraints, the slow displacement speed and the low frequency of use. However such maintenance should be evaluated and this is the task of the nuclear engineering company, which should also consider the radiation hardness of the components.

Two quadrupole lenses placed at each exit of the separator are used to focus the beam at the object point of the secondary beam line optics. It has been found that these lenses had to be placed closer to the electrostatic deflectors than initially forecast. The only way to cope with this constraint is to integrate the electrostatic quadrupole lenses inside the deflector chamber, as shown below, at the expense an increase in the chamber size. Both deflectors and related components are installed on a second platform so that it can be extracted as a whole, as was the case formerly for the deflectors alone. It should be pointed out that the two supports (slit/deflector and quads) are independent.

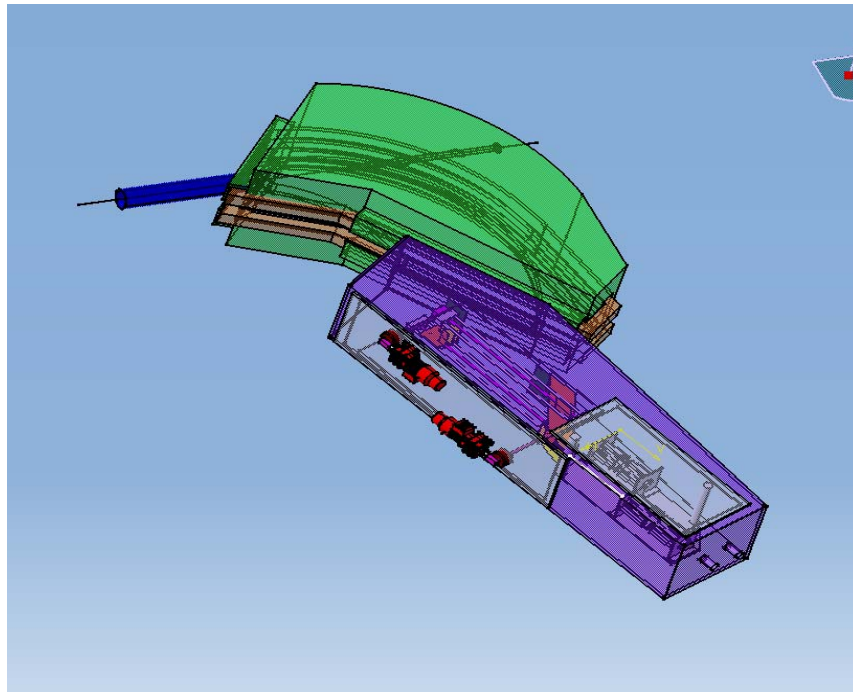


Figure 11: View of BRAMA showing the slit/deflector and quadrupole-lens chamber.

The mechanical constraints and the deformation of both vacuum chambers have been studied and calculated with ACORD 3D. Material properties are based on a non-magnetic stainless steel (ref. X3CrNi18-10) of 15 mm thickness. Due to the external atmospheric pressure and the specific weight the maximum constraint leads to bending of the dipole chamber surface by 2.3 mm. A 1300-l/s Alcatel turbo-molecular pump and a 2000-l/s Coolvac cryopump can provide the 10^{-7} mbar vacuum of the chambers. In Table 3 are shown the relevant dimensions of the chambers.

Table 3: Main characteristics of BRAMA vacuum chambers

	Dimension	Volume
Spectrometer chamber	2 m × 1.5 m × 0.12 m	0.098 m ³
Deflectors and quadrupole chamber	3.3 m × 0.8 m × 0.6 m	1.276 m ³

A small pipe equipped with a glass window in line with and opposite to the entrance pipe of the separator has been added to the spectrometer chamber in order to make provision for the use of a laser ion source.

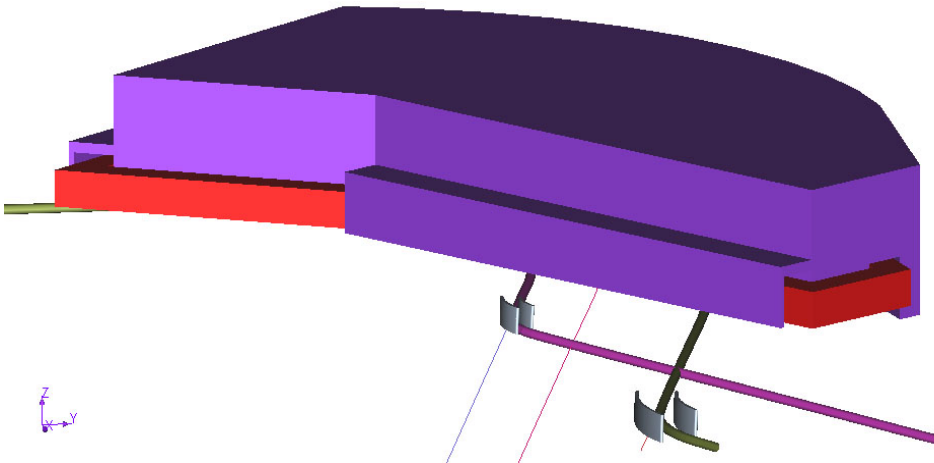
A risk analysis following an FMECA (Failure Modes Effects and Criticality Analysis) process has been performed in order to ensure the integrity of the system. This analysis revealed that the issues previously mentioned, relating to sealing, pumping, lubrication, etc., are as important as the optics of the separator with respect to the nuclear safety aspects. The former can lead to some serious difficulties, whereas the latter can be more-or-less compensated for with the help of the degrees of freedom of the system.

Table 4: Main geometrical characteristics of the Elbek magnetic separator

Parameter	Value
Sector angle	104°
Entrance angle	45°
Exit angle	-38°
Object focal distance	1 m
Image focal distances	0.492 m ($A=70$) to 0.812 m
Curvature radii	0.836 m ($A=70$) to 1.265 m
Gap chamber	100 mm
Magnet weight	20 t (iron) and 0.5 t (copper)
Maximum induction	5 000 Gauss

2.1.2.b. Beam optics design

Beam optical calculations have been performed by tracking particles in a realistic magnetic field calculated by a 3D code, in order to confirm the results previously obtained with first-order codes. Two complementary approaches have been followed, using tracking with (i) ZGOUBI on a TOSCA magnetic field and (ii) LORENTZ, which encompasses both magnetic and electrostatic tracking in a same run, allowing the complete simulation of the 3D geometry of both electric and magnetic fields.

**Figure 12: $A=70$, 100 and 160 amu particle trajectories through the magnetic dipole and electrostatic deflectors.**

The main advantage of this second approach is the possibility of evaluating the perturbations on the beam path outside the devices i.e. to study the behaviour of the beam in the neighbourhood of the components. For example, in the case both electrostatic deflectors (ESDs) are close together, we expect a minimum mass range of 15 amu. For the case $A=100$ and 115 amu (i.e. with the magnet set to the $A=100$ on the central radius), the deformation of the trajectory would reduce the transmission of the $A=115$ amu beam by 30%.

The 36° deflection is provided by 2 electrostatic deflectors with a toroidal shape, enabling focusing in both transverse directions. The applied voltages are ± 10 kV and ± 12.5 kV. Other data characterizing the ESDs are given in Table 5. The mean electric field reaches 5 kV/cm and 2.5 kV/cm respectively, between the electrodes. The most critical points should be located on the edges of the electrodes of the first deflector (ESD1), in front of the slits on the focal plane where the electrical field reaches a value of 10 kV/cm. This rather conservative value presents a large safety factor with respect to the limit fixed by the Paschen curve and other references [6], and should therefore avoid the problems of ionization, field emission and other high-field perturbations.

Table 5: Main data characterizing the toroidal ESDs

	ESD 1	ESD 2
Length (mm)	150	300
Deflection (°)	36	36
Gap (mm)	40	100
Electrode thickness (mm)	10	10
Height (mm)	150	160
Horizontal radius (mm)	239	478
Horizontal/vertical radius ratio*	0.3	0.4
Max. voltage	±10	±12.5
Mean electric field (kV/m)	5	2.5
Distance of focal plane (mm)	127	441

While the detailed LORENTZ calculations are still in progress, for the sake of comparison a ZGOUBI calculation has been performed on a 3D TOSCA map. The results in Figure 13 show the (x,x') and (y,y') phase spaces assuming an 80π mm.mrad emittance. The comparison with the first-order calculation of the focal lengths is shown in Table 6.

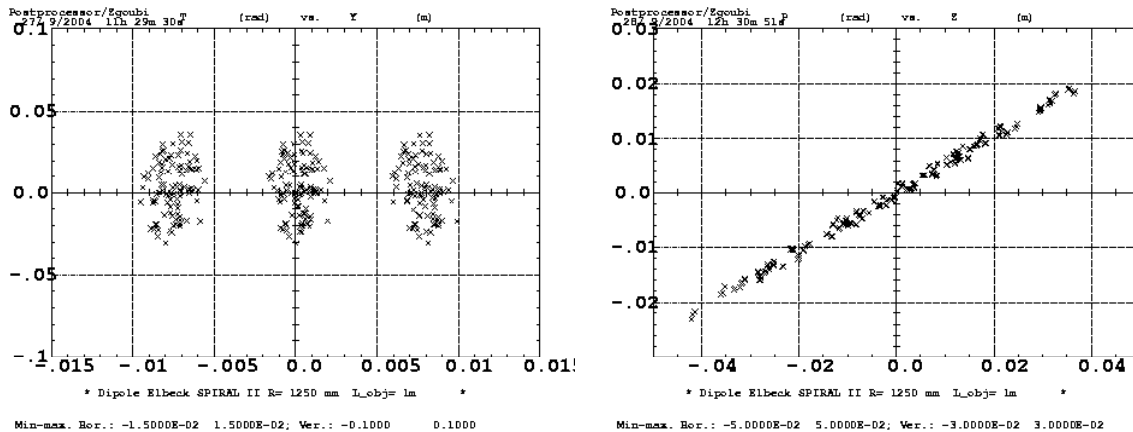


Figure 13: ZGOUBI plots of 3 beams extracted from the BRAMA around 200 amu.

Table 6: Comparison of theoretical and calculated focal lengths.

R (mm)	D GALOPR (mm)	D ZGOUBI (mm)
800	466	439
1000	611	586
1250	800	777
1400	918	900

It can be seen that the first-order properties of the Elbek spectrometer [5] have been confirmed by the tracking calculation. Very few high-order components are present, and if a slight adjustment of the entrance angle might be necessary, the reconstructed first-order matrices are very close to those calculated by TRANSPORT or GALOPR. The position of the focal plane is also very close. Finally, the Elbek spectrometer properties in terms of separation and sensitivity to vertical motion have been fully confirmed by the 3D calculations.

2.1.2.c. Downstream transfer lines

The main goal of lines downstream the BRAMA separator is to deliver the first selected beam to the low-energy physics area and the second one to the charge breeder. These two beams may also be directed to a common identification station. A special implementation of these three lines has been optimized taking into account the specificity of the BRAMA extraction system. Figure 14 presents a schematic view of these beam lines.

All optical elements are electrostatic. There are two main reasons for this. Firstly, these lines transport only singly-charged heavy ions. Their high magnetic and low electric rigidity would involve either high magnetic field gradients or low electric field gradients, respectively. Choosing electrostatic equipment is cost-effective. Secondly the tuning of electrostatic elements is mass-independent. All transport structures – apart from the quadrupoles dedicated to extraction matching – will stay tuned, even if another ion is selected during an experiment. All along the lines, each group of quadrupoles is treated as compact unit, which should ease their maintenance.

The design of the transport lines follows a modular principle. Each line is composed of independent sections making them easier to tune and better suited to implementation of upgrades. Firstly, a complete betatron tuning section appears on each extraction leg from the BRAMA. At its end, a tuning area composed of EMS beam profile monitor and emittance slits provides a total redefinition of the beam. Downstream sections then only provide beam transportation and geometrical guiding. These sections are optically passive, as far as is possible.

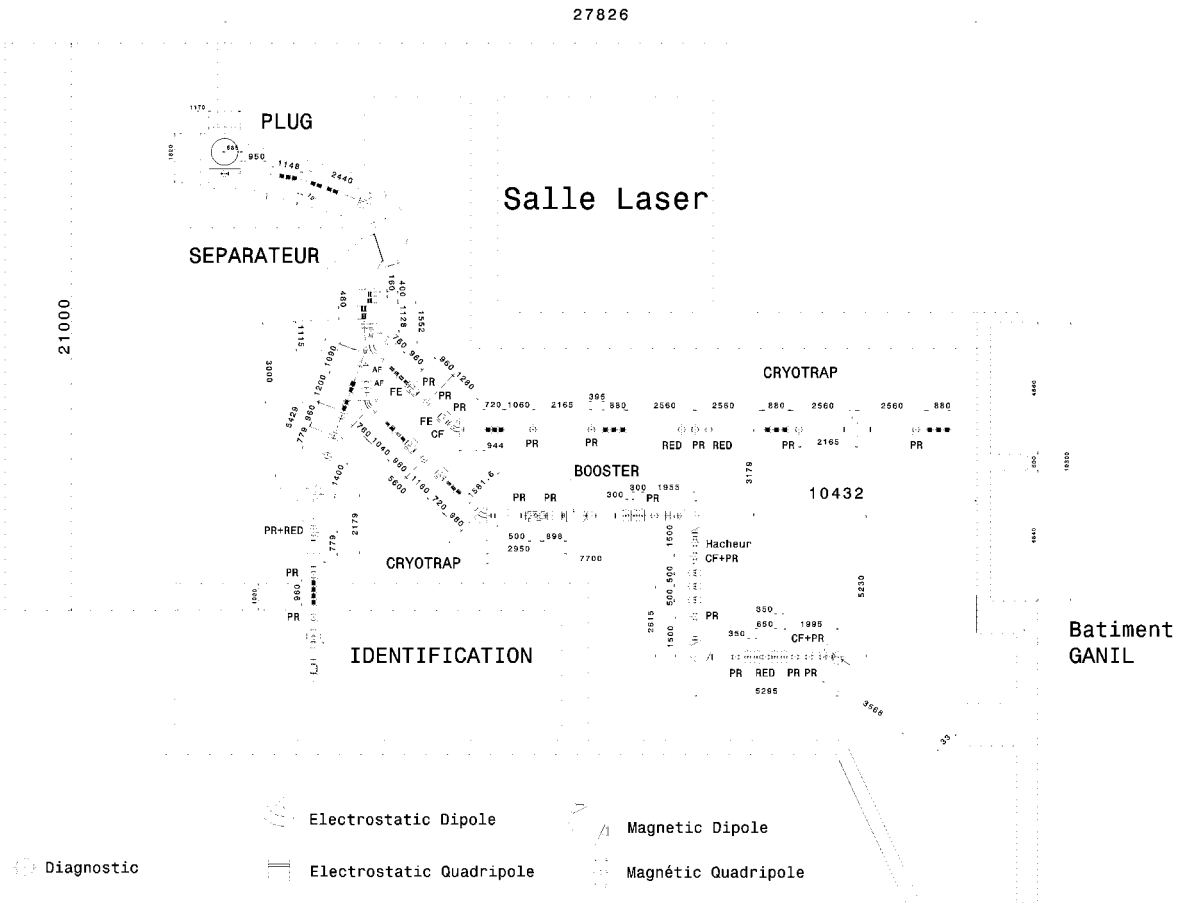


Figure 14: Schematic view of low-energy singly-charged beam line.

The main difficulty encountered in the design of the BRAMA exit, for each of the three lines, is the control of the position of the extraction deflector as function of selected mass. As an example, the drift separating the mobile deflector and the first fixed quadrupole varies between 585 mm and 1493 mm for masses 70 to 160, respectively. To find a good compromise, the optics must be sufficiently versatile to permit simple, sequential tuning through successive-mass beams.

All beam lines must be installed inside a “high nuclear confinement” part of the production building. Particular considerations have to be taken into account during their design. A number of independent pieces of apparatus must be added on these lines to manage the safety risks:

- A “cryotrap” system must disconnect vacuum sections when lines leave the high nuclear confinement area.
- A set of “pepper-pots” must be available for possible reduction of extracted beam intensity.
- A special probe must permit permanent monitoring of the radioactive beam intensity, as it leaves the production building.

All these items of equipment must be placed inside the beam lines and the optics must be designed to satisfy to their requirements.

The line structure at the exit of the BRAMA is composed of a set of two quadrupoles designed to adjust the envelope to compensate for the various positions of the BRAMA deflector. A second beam deflector is located immediately after the first, to spread the two extraction lines. Before it, a set of two small insertable deflectors allows each of the two beams to be directed to the identification station. For each line, four quadrupoles then provide the required betatron matching.

Figure 15 and Figure 16 show the first-order optics which achieves this compromise for the three lines, for extreme masses. On these figures it is possible to observe how the different positions of the extraction deflectors are treated at the exit of the separator. For the selected mass, the six quadrupoles are tuned to obtain an equivalent optical function through the section to permit correct continuity of quadrupoles setting. With the same settings for the first two quads, extraction to the identification line is also realized. The complete dispatching of selected beams to their respective destinations is thus obtained with a really compact mechanical solution, providing an opportunity to limit the areas of radioactive losses. At the end of these sections, beams’ emittance is reduced by sets of slits to match the beam acceptance downstream and to guarantee low-loss transport.

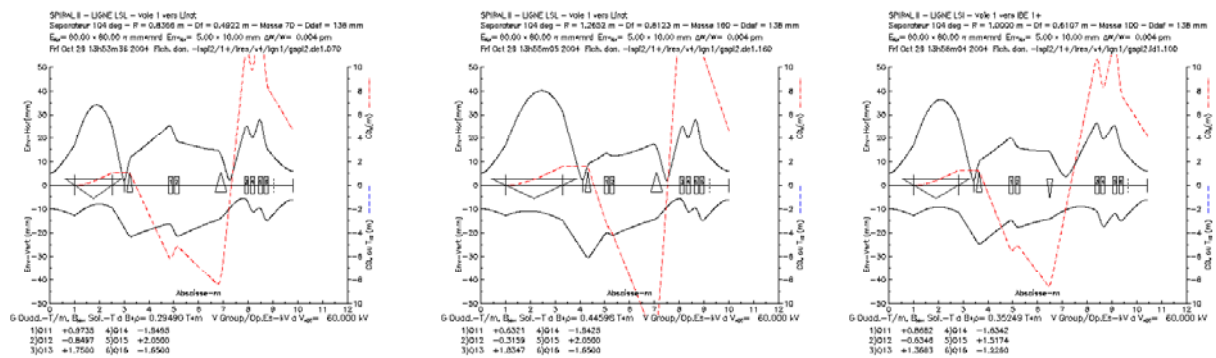


Figure 15: Separator extraction optics for way 1 (interior BRAMA beam line): LSL beam line for mass 70 (left) and 160 (centre) and LSI beam line for mass 100 (right)

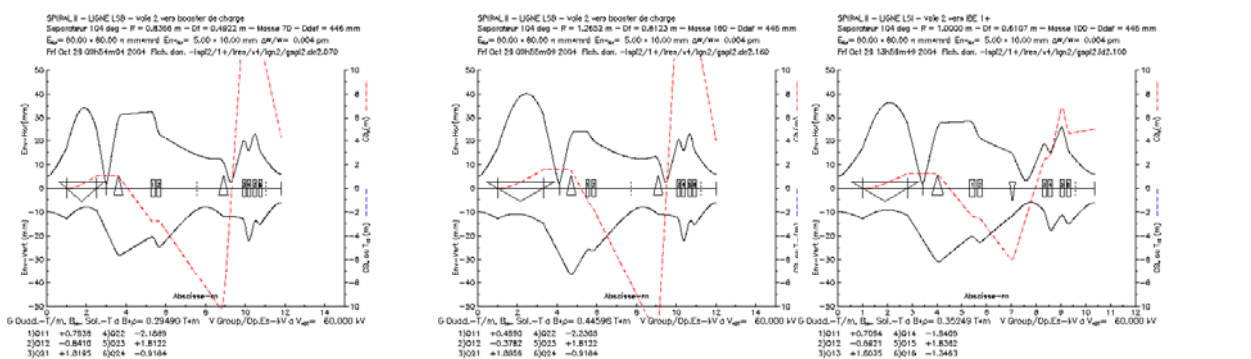


Figure 16: Separator extraction optics for way 2 (exterior BRAMA beam line): LSB beam line for mass 70 (left) and 160 (centre) and LSI beam line for mass 100 (right)

For each of the three beam lines, the downstream sections are simply transportation sections. Their design is based on independent optical structures to guide the beams in as simple a manner as is possible, taking into account the different pieces of equipment to be installed in the lines for nuclear safety. These sections are composed classically with a geometrical deflector for matching and a telescopic system with unit transfer matrix. The matching is mass-independent. Figure 17 shows the first-order optics for these different beam lines.

In each case, final matching depends of necessary conditions downstream. For the LSL beam line, the last six quadrupoles form a section with unit beam transfer matrix. To leave the production building, a repetition of this section will be used. It is possible to introduce cryotrap modules where the beam is small, e.g. between two sets of six quadrupoles. Intensity reduction will take place where the beam is large, e.g. near the middle of six quadrupoles sections.

For LSB beam line, a smooth beam is presented at the breeder entrance. This final section will evolve when we have a better understanding of the necessary conditions. A long free drift section has nevertheless been left to install a cryotrap before the breeder. “Pepper-pots” are preferably reserved for the N+ beam line, after the breeder.

For LSI beam line, long drift sections are also reserved, before the final matching section, to install a cryotrap system and another electrostatic deflector, if necessary, to inject beam coming from a second production cave. “Pepper-pots” can, of course, possibly be implemented in that line also.

It must be however be noted that the transportation sections of these beam lines will again have to be re-examined globally when a better knowledge of building logistics, nuclear safety and interface beam conditions become available. The solutions presented are still provisional proposals to solve the problem of low-energy multi-beam transport.

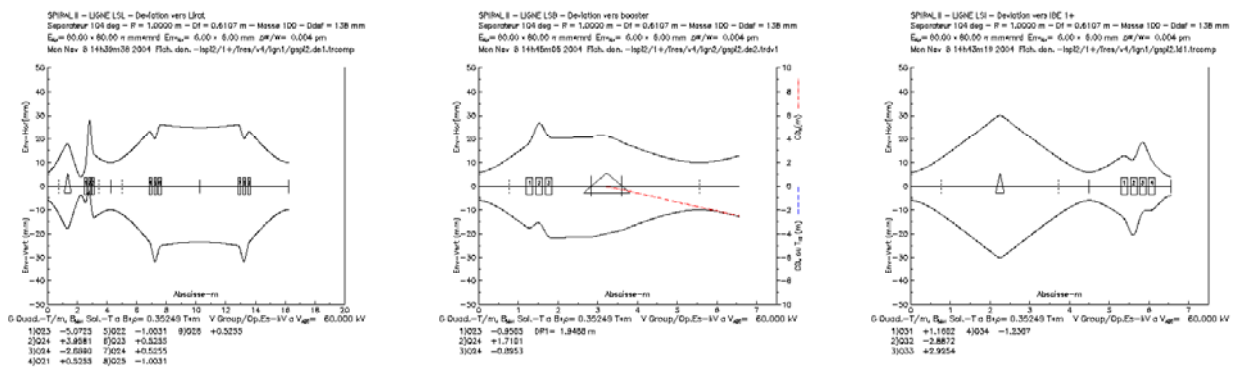


Figure 17: Geometrical transportation optics for LSL (left), LSB (centre) and LSI (right) beam lines

2.2. WIEN FILTER OPTION

The separator should be specially designed to select and transport a continuous beam of ions of a given mass and charge ($A1, q1$) towards the CIME injection line while directing another continuous beam ($A2, q2$) towards the low-energy experimental area. Such a separator must have as wide as possible a range of ions available at the same time for the two beam lines. In addition, the design of the separation system should take account of different constraints, i.e.:

- the large transverse emittance: since a plasma ion source is envisaged, a maximal emittance of 80π mm.mrad is expected;
- the space charge effects: 2mA could be extracted from the plasma source;
- the radioactivity at the exit of target/ion-source system, necessitating a remote-handling system for maintenance and repair.

The feasibility of any beam line and associated spectrometer will be established after the complete evaluation of the repair and maintenance of the equipment. Ideally, the properties of the spectrometer should be:

- a very large acceptance, allowing for the simultaneous use of two beams coming from the peaks of the fission product distribution ($A=90$ and $A=150$); however, this would lead to very large vacuum chamber and magnet.
- selection of 2 isotopes of the same element at the same time, since most of the sources have at least a partial chemical selectivity; but this would lead to the implementation of a moveable electrostatic septum.

The study of any option for the low-energy beam line and separator has to include:

- beam optics calculations (1st-order, space charge, aberrations, etc.);
- mechanical design (remote maintenance, plug manipulation, implantation of diagnostics, compatibility with the design of the hot cell);
- compatibility with safety and radioprotection options and building constraints;
- evaluation of the performance in operation (project goals, flexibility, scientific programme, etc.)

The coherence of all these steps implies a very strong link between the different study groups.

2.2.1. The Wien filter principle

The proposed scheme is based on the decoupling of the functions: the mass separation is performed by a Wien filter [8,9], located in a plug close to the ion source [10], while the mass purification is performed by two independent spectrometers.

A velocity filter allows adjustment of the dispersion, which will separate and transport two masses of interest in two fixed beam lines. Two additional magnetic separators downstream of the velocity filter (one on each beam line) then take care of the final mass purification.

The values of the electric and magnetic fields have to be carefully tuned in order not to deflect the trajectory of the ion dedicated to the cyclotron beam line, while deflecting the ions for the low-energy experimental area through a giving angle towards an electrostatic septum.

The separation of the two beams should be performed before any purification of the beam produced by the target/ion-source system, to retain all possibilities for the choice of the two ion species. Special attention has been taken to minimize the length and the number of components.

The electric and magnetic fields are perpendicular to each other, and the field magnitudes are chosen in such a way that the ion dedicated to the main line follows the central axis, i.e. when the Lorentz force is cancelled. The field magnitudes allow us to send particles of a given mass and charge ($A2, q2$) towards the second beam line.

The deflection angle and position at the exit of the Wien filter can be estimated, and the magnetic and electric fields needed are depicted in Table 7 for different scenarios.

Table 7: Magnetic and electric fields for various mass-separation scenarios

Separation $U_{\text{source}} = 20 \text{ kV}$	$ B $ T	$ E $ (kV/m)	R_{16} m	R_{26} rad
100↔107	0.300	58.9	-0.24	-0.387
100↔110	0.203	39.9	-0.17	-0.282
100↔150	0.050	9.8	-0.04	-0.073
$U_{\text{source}} = 40 \text{ kV}$				
100↔107	0.424	117.9	-0.240	-0.387
100↔110	0.288	79.9	-0.172	-0.282
100↔150	0.070	19.5	-0.044	-0.073

For a Wien filter length $L = 600 \text{ mm}$, a separation $\Delta x = 16.0 \text{ mm}$ is obtained between beam A ($m = 100$; $q = +1$) and beam B ($m = 107, 110$ and 150 ; $q = +1$) for beam energies of 20 and 40 keV.

The Wien filter is thus able to separate ions of closely similar masses. However, the separation limit stems from 3 effects. Thus a high field in the Wien filter:

- a) induces a strong dissymmetry (H-V) in the optics which induces beam losses at the exit of the plug,
- b) increases of the requirement on electric field quality in the Wien filter; and
- c) increases the amplitude of the deviation from the reference trajectory due to non-coherence of the magnetic and electric fringe fields.

These three different effects mean that in practice the separation limit in mass is around 8%. This Wien filter system is thus able to separate a beam of mass m_1 from a beam of mass m_2 included in the ranges:

$$[m_1+8\%, m_1+60\%] < m_2 < [m_1-8\%, m_1-60\%]$$

For the separation of closer masses, we shall consider pulsing the electrode of the Wien filter at a frequency around 1 Hz: if such operating mode is allowed, beam sharing between the two beam lines could be envisaged. For instance, we could imagine directing a beam of mass $m_1=100$ toward the cyclotron during 80% of the beam time, while the low-energy beam line could use a beam with mass $m_2= [m_1-8\%, m_1+8\%]$ during 15% of the beam time.

2.2.2. Space charge studies

Since we want to keep all the different ions (with different masses) in the beam line, we cannot introduce magnetic element at the source extraction. (A solenoid is thus excluded.)

Simulations undertaken with TRANSPORT have shown that a beam with emittance $\varepsilon = 80\pi \text{ mm.mrad}$ and with an intensity $I > 0.5 \text{ mA}$ cannot be transported efficiently with electrostatic quadrupoles. Therefore, we limit ourselves to the use of electrostatic einzel lenses at the extraction of the ion source.

We have to avoid focusing the beam before the suppression of most high-intensity beam components (H^+ , C^+ , O^+ , etc.). Therefore, the first focus is located downstream the Wien filter. The chosen parameters indicate that if the beam is emitted from the source with $x = \pm 2 \text{ mm}$, $x' = \pm 40 \text{ mrad}$ and $E=20 \text{ keV}$, then 1.5 mA of beam current is the maximal achievable value without important beam losses. Indeed, as the intensity increases, it becomes harder to focus the beam after the Wien filter. At higher beam energy, the intensity limit is higher since the generalized perveance K depends on the source voltage:

$$K = \frac{1}{4\pi\epsilon_0\sqrt{2}} \sqrt{\frac{m}{q}} \frac{I}{V_{source}^{3/2}},$$

where K is related to the magnitude of the space charge forces. It is important to notice the strong dependence to the voltage (to the power 3/2). At $V_{source} = 40$ kV (corresponding to a beam energy $E=40$ keV), the intensity limit will be around 4 mA. However important beam losses could occur at the source extraction, if a careful design of the extraction electrode is not undertaken.

2.2.2. Wien filter installation [9]

The Wien filter device will be inserted in a “plug”, similar to the production plug technology, in order to make the maintenance in the radiation environment easier (Figure 18).

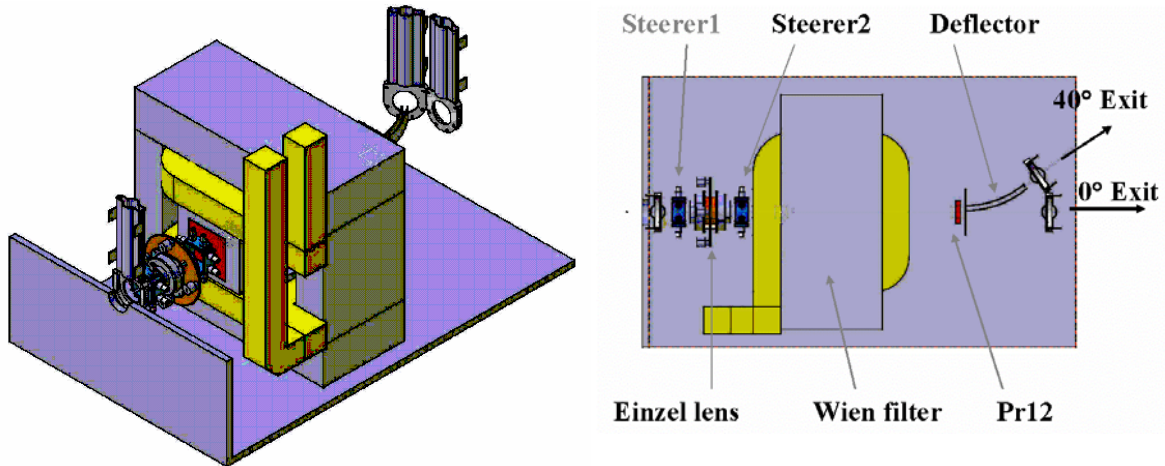
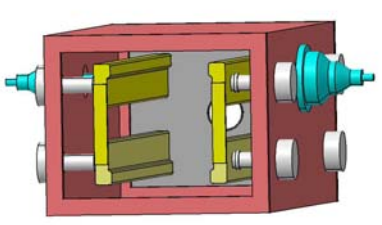


Figure 18: Wien filter plug.

For the design of the electrode, we need to take account for the high intensity of light elements arising from outgassing of the target and/or gas support of the plasma ion source (^{14}N , ^{16}O , ^{12}C , ^{40}Ar , etc.) Such ions can be deflected onto the two sides of the Wien filter. Therefore the “transparency” of the electrodes to such light elements has to be optimized. The main characteristics of the Wien filter are summarized in Table 8.

Figure 19: Electrodes of the Wien filter	Table 8	
		Height
	Length (without coils)	450 mm
	Effective length	600 mm
	Width	1040 mm
	Weight	< 3000 kg
	Inter-electrode distance	160mm
	Magnet gap	250 mm
	B max	0.45 T
	V max	±12 kV

The full beam line includes 20 magnetic quadrupoles, 7 magnets and 1 electrostatic septum. The overall transmission (Wien and spectrometer) is ~70%. The acceptance is 80π mm.mrad and the spectrometer resolution is 1/250. Figure 20 shows the arrangement of the beam lines for the Wien filter option. As before, the identification station can receive the beam from either of the two beam lines.

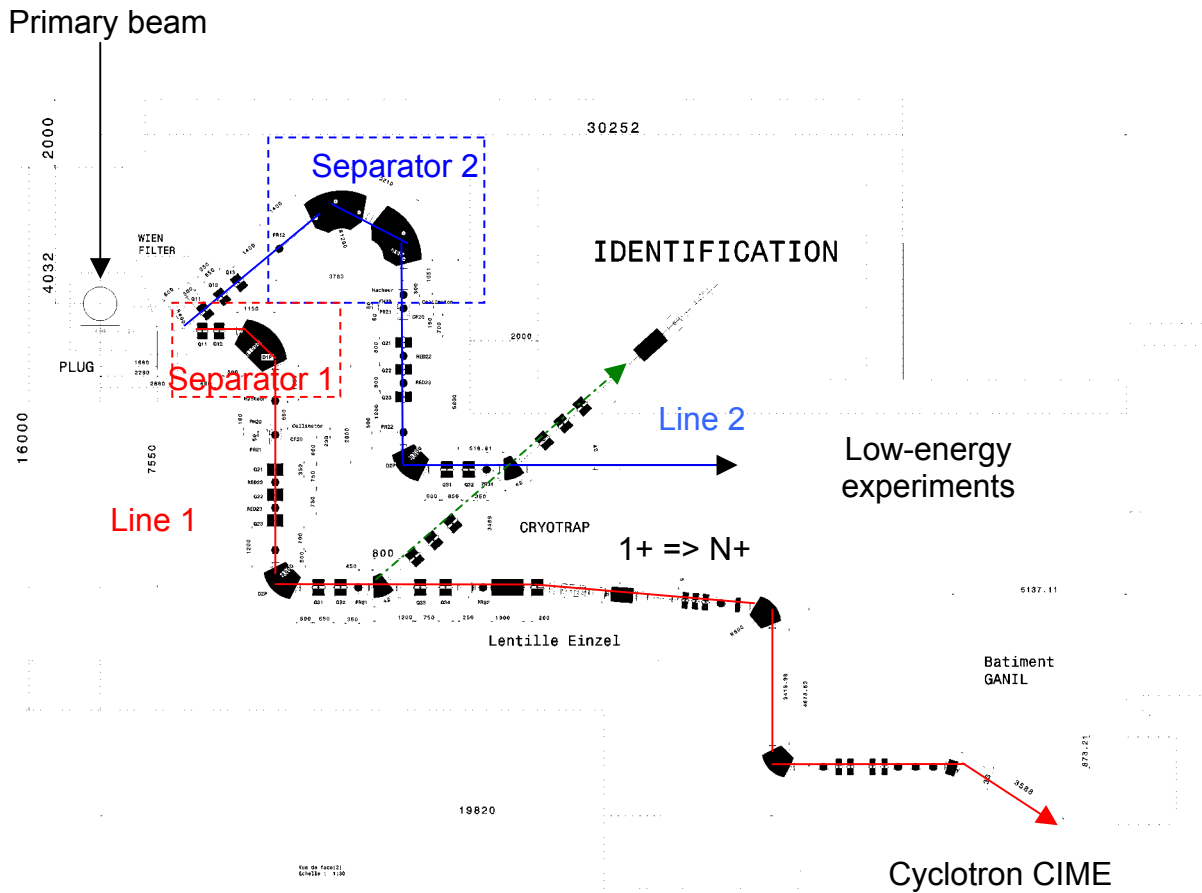


Figure 20: Implementation of the Wien filter option.

Figure 21 shows the beam envelopes for beam line (L1) leading to the CIME cyclotron and for beam line (L2) leading to the low-energy experimental hall.

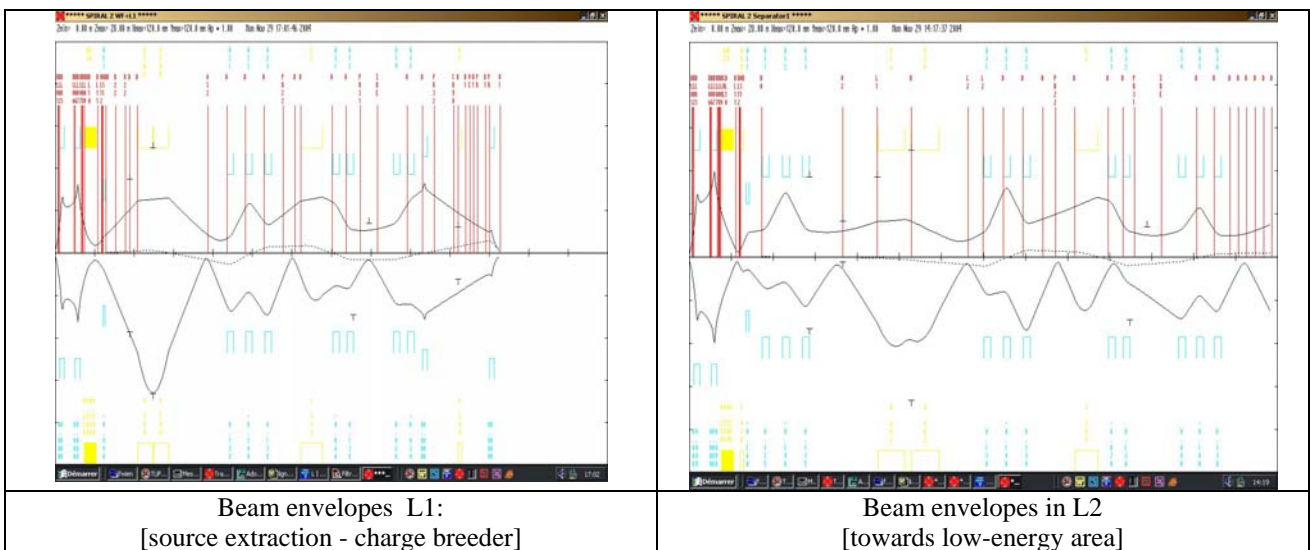


Figure 21: Beam envelopes of L1 and L2 beam lines

The feasibility of such beam lines within the radioactive environment expected has not yet been fully demonstrated. The study has still to be extended to consider the maintenance and repair of components and to evaluate all the consequences. Moreover the location of the identification beam line will be determined by the constraints of the production building. However, this work has led the preliminary design of the Wien filter option and associated beam lines, which has to be considered as a first step. In future, some details should be studied to improve the design are:

- addition of an electrostatic quadrupole before the exit of the plug for more ease in matching of the beam in the line L2;
- optimisation of electrostatic component (protection of the insulators);
- the possibility to insert movable slits or collimators upstream and downstream of the two spectrometers to ensure better beam purification.

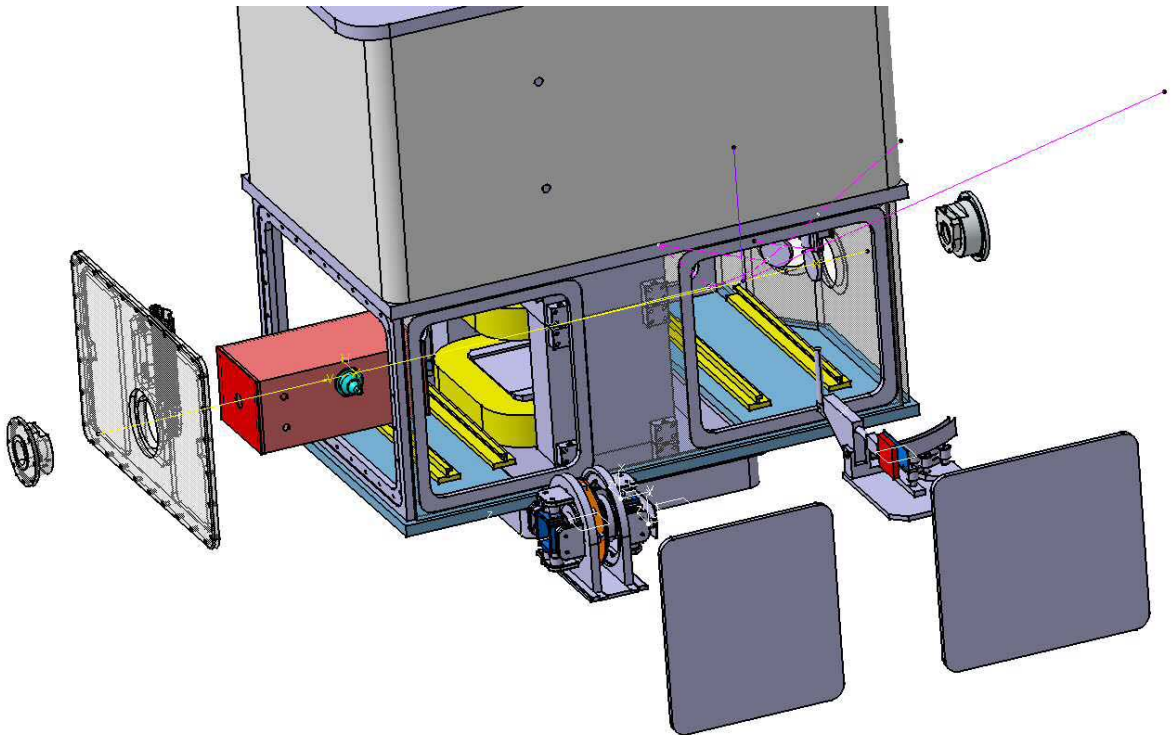


Figure 22: View showing the various different components of the low-energy plug.

3. CHARGE BREEDER

A new test-bench for charge-breeding experiments is now operational at SSI/LPSC/Grenoble and is available for specific SPIRAL II tests. We can use the new MicroPHOENIX 10–18-GHz injection-test source, which can perform low- or high-intensity injection, and also test either singly-charged or multi-charged ion injection. The layout of this test-bench is shown in Figure 23.

Preliminary measurements show a 10% efficiency for the most abundant charge of gaseous ions (1+ to 8+ transformation with argon) and 3% for metallic ions will presumably also be obtained, as on the previous test-bench.

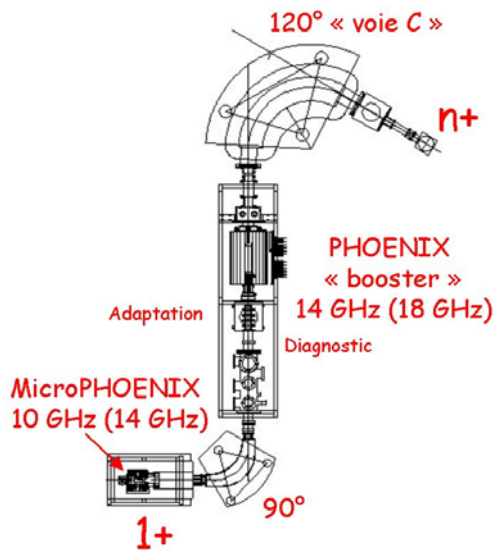


Figure 23: The new test-bench for charge breeding.

For SPIRAL-II specific needs, the LPSC group has worked on a 60-kV design of the booster and on gathering all the data needed for the nuclear engineering company. A view of this design is shown in Figure 24. The nuclear engineering company will propose a maintenance scheme for the booster, since the deposited radioactivity is too high to allow hands-on maintenance, as discussed in the previous report to the TAC.

It should be pointed out that experience at ISOLDE has clearly established the validity of the charge-breeder concept for radioactive beams by extracting a $^{94}\text{Rb}^{15+}$ beam out of a 14-GHz PHOENIX ECR, after the $^{94}\text{Rb}^{1+}$ beam was produced at the ISOLDE target/ion-source. This PHOENIX booster was delivered by PANTECHNIK and is based on a LPSC design.

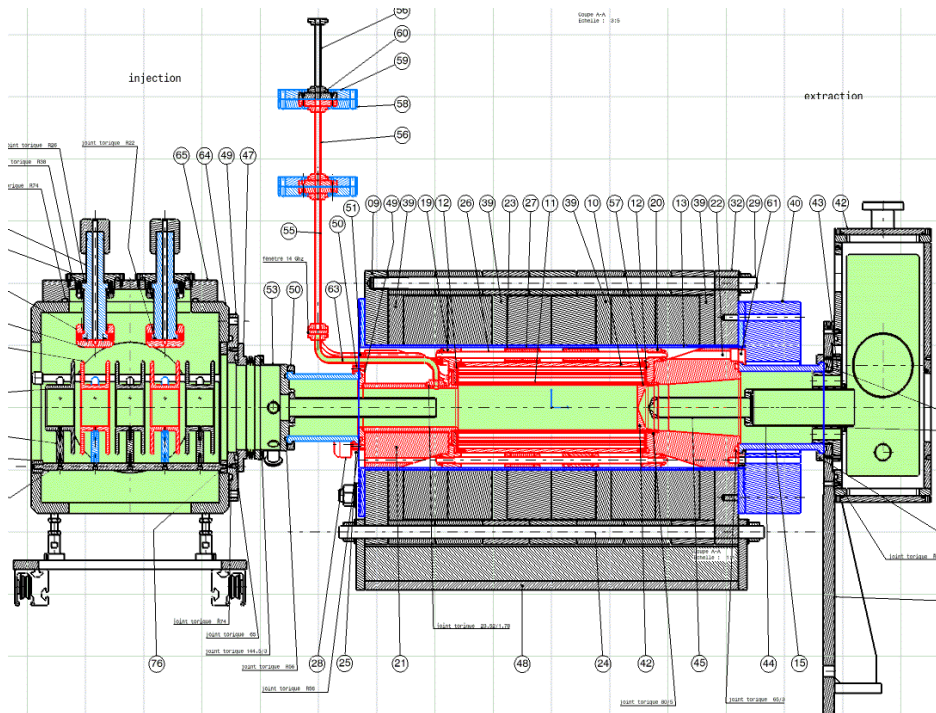


Figure 24: View of the 60-kV version of the charge breeder.

4. MULTI-CHARGED ION BEAM LINE (FROM BOOSTER TO CIME CYCLOTRON)

To post-accelerate low-energy beams emerging from the SPIRAL 2 cave, a long beam line transferring multi-charged ions will have to be constructed between the charge breeder (production building) and CIME (at the north area of the GANIL accelerator building). Beam characteristics of the SPIRAL 2 beam have therefore to be equivalent to those of SPIRAL 1 and a junction point has to be defined. For this purpose, taking account of the structure of the SPIRAL low-energy beam line, we have decided to locate this point at the 'object' point of the CIME injection. The SPIRAL 2 beam must thus be matched to similar conditions at this point. The principle used to design that N+ beam line is to implement a separated-function transfer beam line. Figure 25 shows a schematic view of this line.

This beam line is separated in three main sections, all functionally independent. A first section performs the analysis of the source beam (obtained from the charge breeder), its chromatic compensation and its betatron matching to CIME injection conditions.

A second section provides the physical transportation of this beam through the building. Here we have chosen a structure with a unit transfer matrix (to first order), to achieve reliable low-loss transportation of this fragile beam with relative ease of tuning.

Finally, a modification of the SPIRAL identification line will permit us simultaneously to use the existing station for SPIRAL together with SPIRAL 2 beams, and to deliver the two beams to the CIME cyclotron.

Of course, since the actual position of the charge breeder is not yet fixed, the implementation proposed here must be taken simply as a demonstration of one possibility. The second section of the multi-charged ions beam line will also be adapted to take into account future evolution of the final implementation.

This line has three sections, which are described in detail below.

The first section of the line is itself composed of four subsections. The first one matches the beam to the object point of a classical analysing dipole. A magnetic dipole with low gap to minimize aberrations can be proposed and it needs to prepare the beam with different radial and vertical envelopes. The first piece is designed in this way and is composed of one solenoid and three quadrupoles. It completely decouples the source beam and analyzed one optically. Then, a symmetric classical section performs the analysis and its chromatic compensation with dipoles and quadrupoles. At the end of the section, four quadrupoles perform the required betatron matching.

The second section provides passive transportation of the beam between the two buildings. Two double achromatic deviations, with unit transfer matrix overall, enclose one telescopic, symmetric quadrupole triplet transport section. This section transports the beam, without any change, to the identification room of SPIRAL.

Finally, a third section provides point-to-point transport of the beam symmetrically to the left or right, switching either to the object point of CIME injection, or to the identification station. The low-energy beam line of SPIRAL is modified in the same way, and with the same optics. Figure 26 shows the first order optics of these three sections.

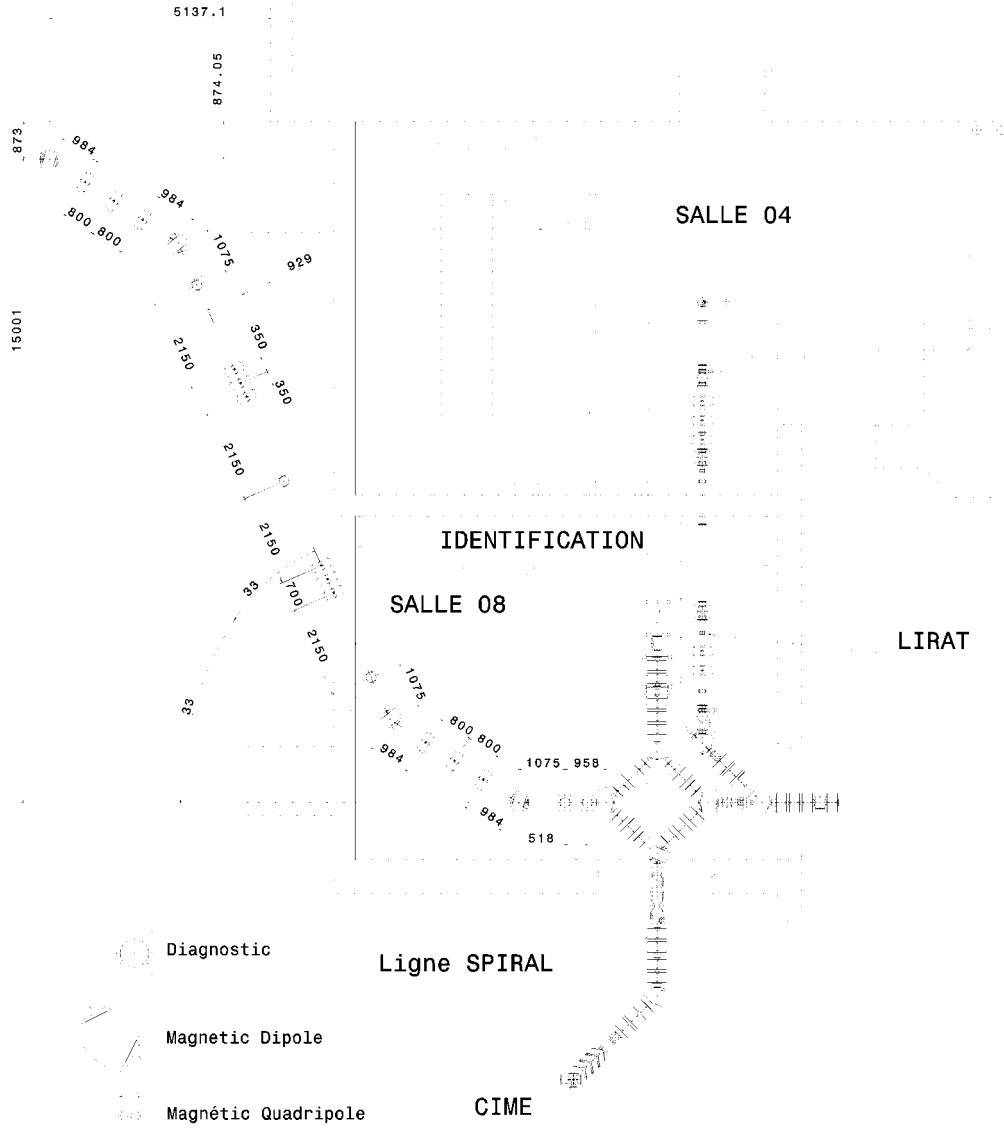


Figure 25: Schematic view of N+ SPIRAL 2 beam line.

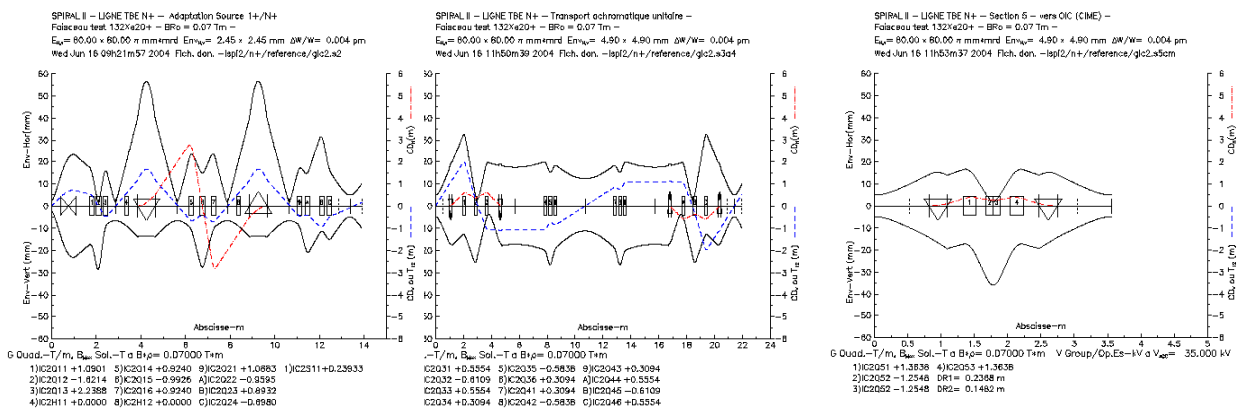


Figure 26: LNP beam line, sections 1, 2 and 3

5. CONCLUSION

At least two solutions are possible for a separator that fulfils the physics requirements. The final choice awaits the input on safety and maintenance from the nuclear engineering company. However, work should still continue on both options. Also, in order to give better estimates of the transmission in the first section in the case of large currents out of the source, the construction of a test-bench for this part is highly desirable to assess the calculated values. It must be stressed that high currents (5mA) are a strong constraint for the separator design.

Furthermore, since the solutions that are needed to comply with the safety requirements may turn out to be too difficult and/or too expensive, a simplified solution has also been considered for each option. The final choice between the two options will be made after input from the nuclear engineering company. We also note that the definition of a beam line is a process with a long maturation time: the optical constraints are generally not the most important ones and the SPIRAL 2 secondary beam lines are no exception.

The layout presented here is thus not a definitive solution, not only because all safety requirements are not yet known but also because the detailed requirements of some equipment in the beam line are also not yet known with sufficient precision.

REFERENCES

- [1] J.M. Nitschke, 'BRAMA, a Broad Range Atomic Mass Analyser for the ISL', Particle Accelerators, 1994, Vol. **47**, pp. 153-158.
- [2] J. Borggreen, B. Elbek, L. Pearch Nielsen, 'A proposed spectrograph for heavy particles', NIM **24** (1963) 21-25.
- [3] Description du séparateur Bi-Sélectif, I-004794
- [4] P. Paris et al., 'Description and performance of the Isocele 2 separator', Proc. 10th EMIS conf., NIM **186** (1981) 61-69.
- [5] H.L Ravn et al., 'New techniques at Isolde-2', NIM **139** (1976) 267-273.
- [6] C. Bruske et al., 'Status report on the GSI on-line mass separator facility', Proc. 10th EMIS conf., NIM **186** (1981) 61-69.
- [7] P. Bertrand, F. Daudin, M. Di Giacomo, B. Ducoudret and M. Duval, 'Improvement of the mass separation power of a cyclotron by using the vertical selection method', XVII International Conference on Cyclotrons and their Applications, Tokyo, Japan, to be published.
- [8] G. Auger, F. Bocage and B. Jacquot, GANIL technical report R00-01.
- [9] R. Cee, 'Beam Optical Calculation for Spiral', GANIL technical report R04-01.
- [10] J.M. Gautier, 'Notes pour l'ingénierie nucléaire : le plug Basse énergie (Option filtre de Wien)', GANIL technical note.